Acta Crystallographica Section B
Structural Science
ISSN 0108-7681

Intersubsystem chemical bonds in the misfit layer compounds $(LaS)_{1.13}TaS_2$ and $(LaS)_{1.14}NbS_2$

Andreas Jobst and Sander van Smaalen*

Laboratory of Crystallography, University of Bayreuth, D-95440 Bayreuth, Germany

Correspondence e-mail: smash@uni-bayreuth.de

Received 6 July 2001
Accepted 12 November 2001

The modulated structures of incommensurate composite crystals $(La_{0.912}S)_{1.13}TaS_2$ at room temperature and of $(La_{0.949}S)_{1.14}NbS_2$ at T = 115 K are refined against high-resolution X-ray data. The compounds are isostructural with superspace group $F'm2m(\alpha,0,0)00s$. For $(LaS)_{1.13}TaS_2$, lattice parameters of the first subsystem TaS_2 were obtained as a = 3.2922 (1), b = 5.7776 (2) and c = 23.013 (2) Å. For the second subsystem LaS, the same b and c parameters were found, but a = 5.8090 (8) Å. Refinements led to a final structure model with R = 0.036 for 4767 observed unique reflections (R = 0.023 for 2147 main reflections, R = 0.099 for 1554 first-order satellites and R = 0.112 for 1042 second-order satellites). The final model includes modulation parameters up to the second-order harmonics for the displacements of the atoms, for the occupational parameters and for the temperature parameters. A clear correlation is found between the relative positions of the subsystems, the displacement modulation, the occupational modulation and the modulation of the temperature parameters. The analysis shows that the variations in environments are resolved by correlated variations in the temperature factors. For $(LaS)_{1.14}NbS_2$, lattice parameters at T = 115 K of the NbS_2 subsystem were obtained as a = 3.3065 (4), b = 5.7960 (5) and c = 22.956 (3) Å. For the LaS subsystem, the same values for b and c were obtained, but a = 5.7983 (7) Å. Refinements led to a final structure model with R = 0.048 for 5909 observed unique reflections (R = 0.034 for 2528 main reflections, R = 0.092 for 2171 first-order satellites and R = 0.113 for 1103 second-order satellites). The final structure model is similar to that of $(LaS)_{1.13}TaS_2$. In particular, it is found that the values of the modulation parameters are almost equal and it is concluded that the modulations are independent of the temperature and the replacement of Ta with Nb, and thus represent a general mechanism of resolving the strain between the mutually incommensurate layers.

1. Introduction

The inorganic misfit layer compounds $(MX)_{1+x}TX_2$, with M = La, Pb, ..., T = Ta, Nb ..., X = S, Se, and $0.07 < x < 0.28$, belong to the class of incommensurate composite crystals (van Smaalen, 1991*a*, 1992*a*; Wiegers, 1996). They comprise alternately stacked layers MX and TX_2 (Fig. 1). Parallel to the layers the lattice constants of MX and TX_2 are equal in one direction (common $\mathbf{b}^*$ axes), while they are mutually incommensurate in the other direction (parallel $\mathbf{a}_1$ and $\mathbf{a}_2$ axes). The $\mathbf{c}^*$ basis vectors are perpendicular to the layers and they are again equal for the two subsystems.

In first approximation the atomic structures can be characterized by two interpenetrating mutually incommensurate

unit cells (Fig. 1). The first unit cell describes the periodic basic structure of the first subsystem TX_2 ($\nu = 1$). This subsystem consists of two closed-packed layers X, which accomodate the metal atoms T in octahedral or trigonal prismatic coordination. The second unit cell describes the periodic basic structure of the second subsystem MX ($\nu = 2$). The MX subsystem has the structure of a distorted two-atom thick (100) slice of a NaCl-type structure.

The true crystal structure involves subsystems with incommensurately modulated structures. The modulation of one subsystem is determined by the periodicity of the other subsystem. The complete structure can be described by the superspace approach with the symmetry given by a (3 + 1)-dimensional superspace group (de Wolff *et al.*, 1981; van Smaalen, 1995).

The inorganic misfit layer compounds are layered materials that show a great variation in their chemistry through the variation of the elements M and T. The misfit layer compounds distinguish themselves from layer compounds in general by the incommensurate contact between the layers

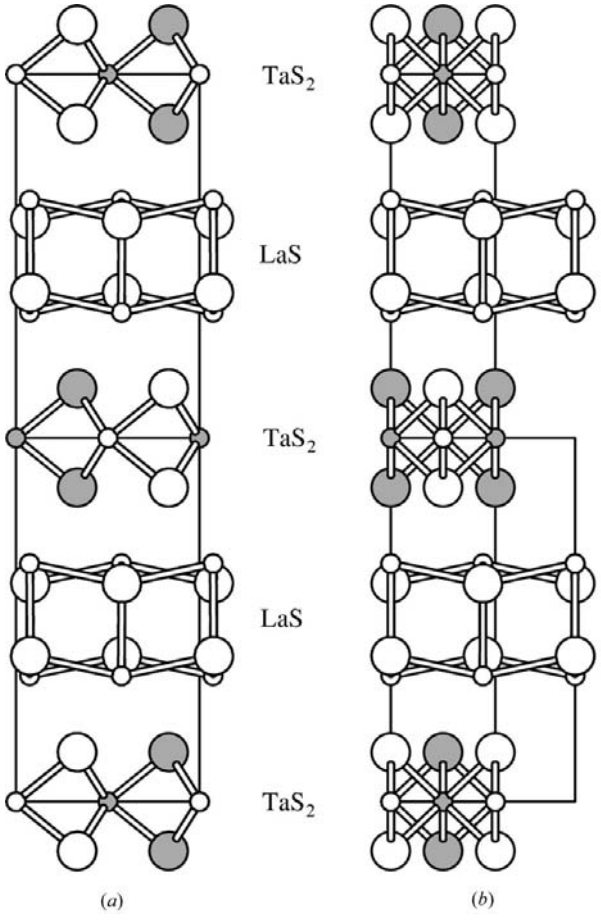

Figure 1
The average structure of $(LaS)_{1.13}TaS_2$. (*a*) Projection along the incommensurate *a* axis; (*b*) projection along the common *b* axis. Large circles denote S atoms, small circles represent the metal atoms. Shaded and white circles represent atoms at different positions of the projected coordinate.

TX_2 and MX, and the question arises towards the consequences of the missing translation symmetry for the physical properties, crystal packing and chemical bonding. It was shown in previous studies that the coordination of the atoms within one compound varies over an infinite number of arrangements. Major variations were that M atoms were bonded towards either one or two S atoms of the other subsystem (van Smaalen, 1995). The modulations were found to make the shortest bond between subsystems (the M to X bond) almost constant, despite the incommensurate nature of this contact. Accordingly, the local structural chemistry was found to vary between limits that were already known from structures on periodic compounds involving the same elements. This normal behaviour was exemplified by the atomic valences as computed by the bond-valence method, which were found to adopt the expected values and to depend only weakly on the incommensurate parameter (van Smaalen, 1992*b*, 1999*a*).

Despite the existing understanding, the true nature of the variations of the chemical bonds has not yet been discovered. It still needs to be determined how the incommensurateness in composite crystals is resolved. Questions to be answered include:

(i) Does the structure comprise domains of ideal commensurate packing, separated by regions of high internal strain, or does a continuous incommensurate variation exist?

(ii) Are the atomic valencies really constant or is there a true variation?

(iii) What are the consequences for the bonding of the variations of the environments of the atoms?

In order to provide answers to these questions, we have performed high-resolution X-ray scattering experiments on the inorganic misfit layer compounds $(LaS)_{1.13}TaS_2$ and $(LaS)_{1.14}NbS_2$. $(LaS)_{1.13}TaS_2$ was first synthesized by de Boer *et al.* (1991), but only the periodic basic structures of the subsystems were determined. The modulated structure at room temperature of $(LaS)_{1.14}NbS_2$ was studied previously (van Smaalen, 1991*b*; Meerschaut *et al.*, 1989). A structure model was developed consisting of a basic structure and modulation functions up to the second harmonic for the displacements of the atoms. For the present study we have measured much more extensive data sets. This allows us to show that the continuous variations in the local environments are a true property of these compounds. It is found that these variations led to variations in the temperature factors. That is, more tight environments with higher valence values are found to correspond to less extensive distributions of the positions of the atoms (smaller temperature factors). Finally, persuasive evidence is obtained concerning vacancies on the La atomic sites, as was originally suggested by Rouxel *et al.* (1994) for similar misfit layer compounds. We find that the modulation of the occupancy of the La atomic site is correlated with the variations in the environment of this site, such that sites with higher valencies have higher occupancies. This can be interpreted by the assumption that sites with more bonding attract atoms, while vacancies preferably occur for the less bonded sites.

2. Superspace description

The superspace description of $(LaS)_{1.14}NbS_2$ has been discussed previously (van Smaalen, 1991*b*; Janssen *et al.*, 1999). $(LaS)_{1.13}TaS_2$ and $(LaS)_{1.14}NbS_2$ are isostructural and thus their superspace descriptions are equal.

Bragg reflections are indexed with respect to a set of four reciprocal basis vectors $M^* = \{\mathbf{a}_1^*, \mathbf{a}_2^*, \mathbf{a}_3^*, \mathbf{a}_4^*\}$, according to

$$\mathbf{H} = H\mathbf{a}_1^* + K\mathbf{a}_2^* + L\mathbf{a}_3^* + M\mathbf{a}_4^* \qquad (1)$$

with $\mathbf{a}_4^* = \sigma_1\mathbf{a}_1^*$, $\sigma_1 = 0.5667$ for $(LaS)_{1.13}TaS_2$ and $\sigma_1 = 0.5703$ for $(LaS)_{1.14}NbS_2$ (see §3). With this choice of basis vectors, the general reflection conditions $H + K + M = 2n$, $H + L = 2n$ and $K + L + M = 2n$ for the (H, K, L, M) reflections were observed. They correspond to the centering translations

$$\begin{pmatrix} 1/2 & 1/2 & 0 & 1/2 \\ 1/2 & 0 & 1/2 & 0 \\ 0 & 1/2 & 1/2 & 1/2 \end{pmatrix}. \qquad (2)$$

This represents a non-standard centering in superspace with the tentative symbol F'. The superspace group was found as $F'm2m(\sigma_1, 0, 0)00s$. The symmetry operators, including the origin-dependent translation components, are

$$\begin{matrix} x_1, & x_2, & x_3, & x_4 \\ x_1, & x_2, & -x_3, & 1/2 + x_4 \\ -x_1, & x_2, & x_3, & -x_4 \\ -x_1, & x_2, & -x_3, & 1/2 - x_4 \end{matrix}. \qquad (3)$$

The reciprocal lattices of the two subsystems ($\nu = 1, 2$), as well as the modulation wavevectors of the subsystems, are obtained from $\boldsymbol{M}^*$ by application of 4×4 integer matrices $\boldsymbol{W}^\nu$ (van Smaalen, 1995). The matrix $\boldsymbol{W}^1$ was chosen as the unit matrix. For the second subsystem the $\boldsymbol{W}$ matrix is

$$W^2 = \begin{pmatrix} 0 & 0 & 0 & 1 \\ 0 & 1 & 0 & 0 \\ 0 & 0 & 1 & 0 \\ 1 & 0 & 0 & 0 \end{pmatrix}. \qquad (4)$$

The $\boldsymbol{W}^\nu$ matrices represent coordinate transformations in superspace. Accordingly, they can be used to transform the superspace coordinates or symmetry operators. Thus, the subsystem superspace groups $G_s^1 = F'm2m(\sigma_{11}, 0, 0)00s$ and $G_s^2 = C'm2a(\sigma_{21}, 0, 0)000$ are obtained. The space groups describing the symmetries of the basic structures of the subsystems are $Fm2m$ for TaS_2 and NbS_2 and $Cm2a$ for LaS. It is noticed that the standard setting of the $Cm2a$ space is obtained when a c axis half the length of $\mathbf{a}_{23}$ is used (van Smaalen, 1991*a*). From (4) it follows that the reciprocal basis vectors $\mathbf{b}^*$ and $\mathbf{c}^*$ are common to the subsystems, whereas $\mathbf{a}^*$ of subsystem $\nu = 1$ provides the modulation wavevector for subsystem 2 and $\mathbf{a}_2^* = \mathbf{q}^1$. It thus follows that $\sigma_1 = a_1/a_2$. The coordinates of the modulation wavevectors relative to the reciprocal basis vectors of the same subsystem are

$$\sigma_{11} = \sigma_1 \qquad \sigma_{21} = 1/\sigma_1. \qquad (5)$$

The reflections can be divided into the following groups:

$(H, K, L, 0)$: main reflections of subsystem 1;

$(0, K, L, M)$: main reflections of subsystem 2;

$(0, K, L, 0)$: common main reflections;

(H, K, L, M) with $H \neq 0$ and $M \neq 0$: satellite reflections.

The satellite reflections can be interpreted as satellites of subsystem 1 of the order $|M|$ and as satellites of subsystem 2 of the order $|H|$. Accordingly, the main reflections of subsystem 1 are at the same time satellites of the second subsystem of the order $|H|$ and the main reflections of subsystem 2 are at the same time satellites of the first subsystem of the order $|M|$.

For the definition of the coordinates, temperature parameters, occupation parameters and their modulation parameters, see van Smaalen (1995).

3. Experimental

3.1. Synthesis and X-ray scattering

$(LaS)_{1.13}TaS_2$ and $(LaS)_{1.14}NbS_2$ were synthesized by heating a stoichiometric mixture of the elements in evacuated quartz-glass ampoules at T = 1073 and 1323 K, respectively (Wiegers *et al.*, 1990; de Boer *et al.*, 1991; Wiegers, 1996). Single crystals were grown by gas transport in evacuated quartz-glass ampoules starting with 300 mg from the previously synthesized powders and 10 mg of $(NH_4)_2PbCl_6$ as the transport agent (Wiegers, 1996). Temperature gradients of 1373–1163 K for $(LaS)_{1.13}TaS_2$ and 1383–1033 K for $(LaS)_{1.14}NbS_2$ were used. Shiny dark grey plate-like single crystals of sizes up to 5 mm were obtained at the low-temperature sides. The plate-like crystals were often found intergrown with each other. For the X-ray experiments only isolated plates were selected, which had the appearance of true single crystals.

The crystals can be divided into two types. The first type consists of the thinner plates, with a thickness of approximately 10 µm or less, which is almost independent of the lateral dimensions of the crystals. Sizes of up to 5 mm were found. The second type consists of the thicker platelets with a thickness that is proportional to the lateral dimensions. Sizes of these crystals vary between $0.01 \times 0.1 \times 0.1$ and $0.05 \times 1.0 \times 1.0$ mm^3.

Many crystals of both types and both compounds were tested by X-ray scattering. Significant differences in lattice parameters between different specimens were not found. However, there was a great variation in the amount of diffuse scattering and for some crystals twinning was observed. Taking the absence of diffuse scattering and twinning as a measure for crystal quality, two trends were observed:

(i) For both compounds, the thicker crystals had a higher quality than the thinner ones.

(ii) The crystals of $(LaS)_{1.14}NbS_2$ had a higher quality, than crystals of $(LaS)_{1.13}TaS_2$.

The twins that we have observed are related by a rotation about **c** over an angle of 60 or 120°. Their existence can be rationalized in terms of the pseudo-hexagonal lattice of the TS_2 subsystems (Kuypers & van Landuyt, 1992). Diffuse scattering was found to be concentrated in circles in reciprocal space (Fig. 2), that might indicate a two-dimensional powder-

Table 1
Experimental details.

	(I)	(II)
Chemical formula	$(LaS)_{1.13}TaS_2$	$(LaS)_{1.14}NbS_2$
Chemical formula weight	438.26	351.93
Temperature (K)	293	115
Crystal form	Plate	Plate
Crystal size (mm^3)	$0.15 \times 0.20 \times 0.03$	$0.15 \times 0.12 \times 0.05$
Crystal colour	Dark grey metallic	Dark grey metallic
Cell setting	Orthorhombic	Orthorhombic
Superspace group	$F'm2m(\alpha, 0, 0)00s$	$F'm2m(\alpha, 0, 0)00s$
Subsystem 1†	TaS_2	NbS_2
a (Å)	3.2922 (1)	3.3065 (4)
b (Å)	5.7776 (2)	5.7960 (5)
c (Å)	23.013 (2)	22.956 (3)
Modulation wavevector	(0.5667, 0, 0)	(0.5703, 0, 0)
Z	4	4
Subsystem 2	LaS	LaS
a (Å)	5.8090 (8)	5.7983 (7)
b (Å)	5.7777 (2)	5.7960 (5)
c (Å)	23.014 (2)	22.958 (2)
Modulation wavevector	(1.7645, 0, 0)	(1.7536, 0, 0)
Z	8	8
D_{calc} (g cm^{-3})	6.648	5.311
Diffractometer	Nonius Mach3 with rotating anode	Nonius Mach3 with rotating anode
Detector	Scintilation counter	Scintilation counter
Radiation type	Mo $K\bar{\alpha}$	Mo $K\bar{\alpha}$
Wavelength (Å)	0.71073	0.71073
Data collection method	$\omega/2\theta$ scan	$\omega/2\theta$ scan
θ-Range (deg)	1.65–45.06	1.73–46.14
Scan width (°)	$\Delta\omega = 1.2 + 0.35\tan(\theta)$	$\Delta\omega = 1.2 + 0.35\tan(\theta)$
Scan speed (° min^{-1})	1.37	2.06
Range of (h, k, l, m)	$-7 \le h \le 7$ $-11 \le k \le 11$ $0 \le l \le 45$ $-15 \le m \le 15$	$-7 \le h \le 7$ $-11 \le k \le 11$ $0 \le l \le 45$ $-15 \le m \le 15$
No. of measured reflections	17 900, 8437	20 950, 10 814
No. of independent reflections		
All	9037, 4767	10 379, 5909
Main	2256, 2147	2573, 2528
Subsystem 1	724, 724	837, 837
Subsystem 2	1336, 1227	1526, 1481
Common	196, 196	210, 210
Satellites ($m = 1$)	3687, 1554	4223, 2171
Satellites ($m = 2$)	3069, 1042	2441, 1103
Criterion for observed reflections	$I > 3\sigma(I)$	$I > 3\sigma(I)$
R_{int} (obs,all)	0.010, 0.007	0.013, 0.009
Absorption correction	ψ scans, *HABITUS* (Herrendorf, 1993)	ψ scans, *HABITUS* (Herrendorf, 1993)
μ (mm^{-1})	37.0	14.7
Min. and max. correction	2.25, 28.42	2.08, 4.14
Refinement on	F	F
$\Delta f', f''$ Ta	−0.705, 6.523	−0.705, 6.523
$\Delta f', f''$ Nb	−2.073, 0.622	−2.073, 0.622
$\Delta f', f''$ La	−0.287, 2.452	−0.287, 2.452
$\Delta f', f''$ S	0.125, 0.123	0.125, 0.123
R, wR (all reflections)	0.072, 0.072	0.091, 0.086
S	1.91	2.28
No. of parameters	66	60
Weighting scheme	$1/[\sigma^2(F) + (0.018F)^2]$	$1/[\sigma^2(F) + (0.020F)^2]$
Extinction correction	Isotropic type I (Becker & Coppens, 1974)	Isotropic type I (Becker & Coppens, 1974)
Extinction coefficient	0.051 (2)	0.078 (4)

† The description of the first subsystem also provides canonical superspace, because W^1 is the unit matrix.

like disorder in these specimens. A detailed analysis of the diffuse scattering will be given elsewhere (Jobst & van Smaalen, 2001). For the present data collections and structural analyses one crystal of each compound was selected from the thicker type, which did not show diffuse scattering or twinning.

X-ray scattering experiments were performed on a Nonius MACH3 four-circle diffractometer with a scintillation counter and a rotating anode source. X-ray scattering of $(LaS)_{1.13}TaS_2$ was measured at room temperature. For $(LaS)_{1.14}NbS_2$ a measurement was made at $T = 115$ K. A Nonius nitrogen gas-stream cryostat was used. In each case lattice parameters were determined independently for each subsystem from the setting angles of four different settings of 25 main reflections of that subsystem.

Integrated intensities were measured for the main reflections and for the satellite reflections up to the order $|2|$. This means that all reflections (H, K, L, M) were measured, for which either $|H| \le 2$ or $|M| \le 2$ (or both conditions were fulfilled simultaneously). Three main reflections of the TS_2 subsystem were measured every hour as reference reflections. The intensities of the reflections were corrected for the variation of the intensities of the reference reflections, and for Lorentz and polarization effects, using the computer program *HELENA* (Meetsma & Spek, 1996). Crystal shapes for the absorption correction were determined by optimization against ψ scans of reflections of the TS_2 subsystem by the computer program *HABITUS* (Herrendorf, 1993). Data sets for the refinements were obtained by averaging the intensities according to the acentric point symmetries. In this way the effects of anomalous dispersion could be taken into acount. The experimental details are given in Table 1.[1]

3.2. Structure refinements

All structure refinements were made using the computer program *JANA*98 (Petříček & Dušek, 1998).

[1] Supplementary data for this paper are available from the IUCr electronic archives (Reference: CK0009). Services for accessing these data are described at the back of the journal.

Table 2
R values for the refinement of Model A and Model B for $(LaS)_{1.13}TaS_2$.

	Model A		Model B	
Reflection group	*R*(obs)	*wR*(obs)	*R*(obs)	*wR*(obs)
All	0.056	0.107	0.036	0.068
Main	0.035	0.050	0.023	0.035
Main (TaS_2)	0.031	0.035	0.015	0.020
Main (LaS)	0.039	0.059	0.030	0.043
Common	0.043	0.060	0.036	0.045
Satellites $m = 1$	0.157	0.185	0.099	0.125
Satellites $m = 2$	0.179	0.258	0.112	0.137

The starting values for the coordinates of the basic structure were taken from van Smaalen (1991*b*). The first step was to refine the basic structure coordinates and anisotropic temperature parameters against the main reflections. The main reflections of one subsystem are satellites of the other subsystem and thus contain information about the modulation. In the second step the amplitudes of La for the displacive modulation were refined, still using main reflections only. In each case, starting values for modulation parameters were taken as arbitrary but small numbers. In the third step all parameters for the displacive modulation were refined against the complete data including satellite reflections. The result of this refinement for $(LaS)_{1.13}TaS_2$ is denoted as 'Model A', while the result for $(LaS)_{1.14}NbS_2$ is denoted as 'Model C'. These models correspond to the final structure model that was obtained in the previous study on the room-temperature structure of $(LaS)_{1.14}NbS_2$ (van Smaalen, 1991*a*). In further steps, modulation functions for the temperature parameters and for the occupancies were introduced. The best structure models and the corresponding refinements are denoted by 'Model B' for $(LaS)_{1.13}TaS_2$ and by 'Model D' for $(LaS)_{1.14}NbS_2$.

The incommensurate composite character implies that the Bragg reflections can be uniquely indexed by the four integers (H, K, L, M), see (1). However, different reflections might have arbitrary close scattering vectors, when arbitrarily high indices are allowed, and overlap of reflections is an intrinsic problem for the X-ray analysis of composite crystals.

For both compounds the value of σ_1 differs only slightly from $\frac{4}{7}$, and a reflection (H, K, L, M) is close to reflections with the indices $(H \pm 4, K, L, M \mp 7)$. This would become a problem only if both reflections are a main reflection or at least a low-order satellite. For example, $(4, K, L, 0)$ is close to $(0, K, L, 7)$, while the intensity of $(8, K, L, -7)$ can be neglected. However, the centering F' implies that one of the two low-index reflections is always extinct and the problem of overlapping reflections does not exist at this level.

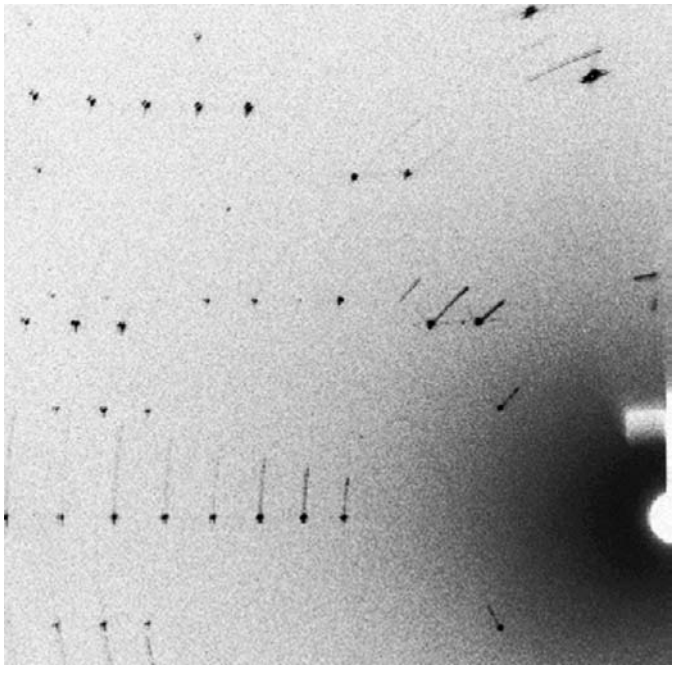

Figure 2
Rotation photograph of a crystal of $(LaS)_{1.13}TaS_2$. The crystal was rotated around the incommensurate **a** axis. The diffuse scattering which can be observed is concentrated on sectors of rings in the reciprocal lattice.

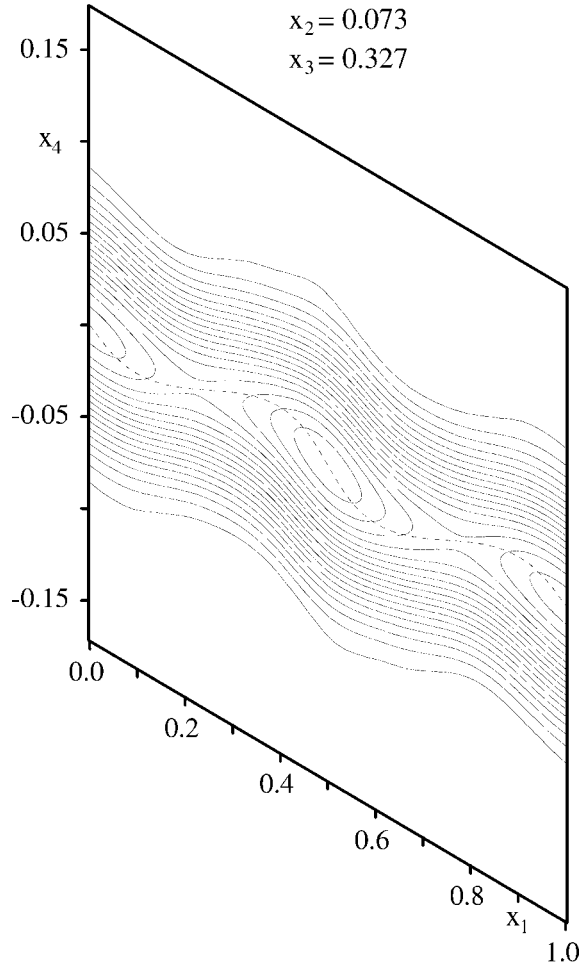

Figure 3
(x_1, x_4) section of the Fourier map of $(LaS)_{1.13}TaS_2$ at the position of La2. Reflection phases were obtained from the refinement with Model A. The contours are at intervals of 25 e Å^{-3}. The dashed line shows the positon of La in the model.

Table 3
Minimum and maximum values in the Fourier maps (ρ in e Å^{-3}) and difference Fourier maps ($\Delta\rho$ in e Å^{-3}) of $(LaS)_{1.13}TaS_2$.

Shown are the results for F_{calc} obtained for Model A and Model B. The Fourier maps and difference Fourier maps were calculated for a cube of (2 Å)^3 around the atom that is indicated and for $t = 0$ to $t = 1$. Positive values in the difference Fourier map indicate an excess of electrons.

		Model A		Model B	
		Min	Max	Min	Max
Cell	ρ	−44.4	987.1	−37.4	914.9
	$\Delta\rho$	−69.5	71.6	−12.6	11.3
Ta1	ρ	−43.2	987.1	−36.5	914.9
	$\Delta\rho$	−8.6	27.2	−5.0	5.8
S1	ρ	−21.6	149.0	−19.7	138.0
	$\Delta\rho$	−4.7	6.1	−3.8	2.9
La2	ρ	−20.9	497.9	−23.5	481.5
	$\Delta\rho$	−69.5	71.6	−12.6	11.3
S2	ρ	−12.1	109.0	−10.8	97.8
	$\Delta\rho$	−6.7	5.3	−5.0	3.0

Alternatively, the reflection (H, K, L, M) is also close to the reflections $(H \pm 8, K, L, M \mp 14)$ and both reflections are present or extinct simultaneously. Overlap of the experimental intensities might thus occur. As before, the problem only exists if two of the three reflections are both low-index reflections. For example, the main reflections $(8, K, L, 0)$ and $(0, K, L, 14)$ fulfil this condition. It turns out that the scattering vectors of these reflections are beyond the maximum scattering angle of our experiment. Instead, our data sets contain main reflections of the type $(-6, K, L, 0)$, which are close to second-order satellites of the second subsystem $(2, K, L, -14)$. The refinements showed that the calculated intensities for these satellites were systematically too low and we attribute this to the fact that the measured intensities of these satellites contain part of the intensity of the nearby main reflection. For this reason, all satellites $(2, K, L, -14)$ were excluded from the final refinements. No such problem occurred with the $(6, K, L, 0)$ main reflections and they were used in all refinements.

3.2.1. $(LaS)_{1.13}TaS_2$. The standard description of the modulated structure with displacive modulations up to the second harmonic (Model A) gives a good fit to the main reflections, but a relatively poor fit to the satellites (Table 2). The deficiencies in Model A become obvious from the Fourier map and the difference Fourier (Figs. 3 and 4). The Fourier map nicely shows the modulation of the La atoms, but the calculated position of La does not exactly follow the trace of maximum density. The difference Fourier is highly structured with maximum and minimum values of $\Delta\rho$ up to 10% of the density at the position of La2 (Table 3). This shows that Model A does not describe all aspects of the structure and that the X-ray data contain information to derive an extended structure model.

Closer inspection of the Fourier map at the position of La2 shows that the width of the electron distribution perpendicular to the x_1 axis (that is in physical space) varies as a function of x_4, when it is measured between contours of equal density (Fig. 3). Owing to the lower electron density of the S atoms and the smaller modulation amplitudes of Ta1, this effect was only clearly seen for La2. Possible reasons for this variation include a modulation of the occupancies and a modulation of the temperature parameters. Therefore, we have introduced modulation parameters up to the second harmonic for the temperature parameters of La2 and Ta1. A clear improvement of the fit to the satellites was observed, with partial R values of 0.101 for the first-order satellites and 0.134 for the second-order satellites. Modulation parameters for the temperature factors of S1 and S2 did not lead to lower R factors, and these parameters remained small and less than their standard

Table 4
Displacement modulation parameters for Model B of $(LaS)_{1.13}TaS_2$.

Shown are the amplitudes A_{ni} and B_{ni} multiplied by the corresponding lattice parameter a_{vi} (Å). $A_{n2} = A_{n3} = B_{n1} = 0$ (n = 1, 2), as determined by symmetry.

	$a_{v1}B_{11}$	$a_{v2}A_{12}$	$a_{v3}A_{13}$	$a_{v1}B_{21}$	$a_{v2}A_{22}$	$a_{v3}A_{23}$
Ta1	0	0.0091 (1)	0	0.02480 (9)	0	0.0073 (1)
S1	0.0265 (9)	0.0111 (5)	0.0064 (9)	0.0341 (5)	0.0072 (7)	0.0249 (6)
La2	0.0170 (5)	0.0895 (2)	0.0281 (3)	0.0544 (3)	0.0082 (6)	0.0060 (4)
S2	0.018 (1)	0.0511 (7)	0.009 (1)	0.018 (1)	0.011 (2)	0.008 (1)

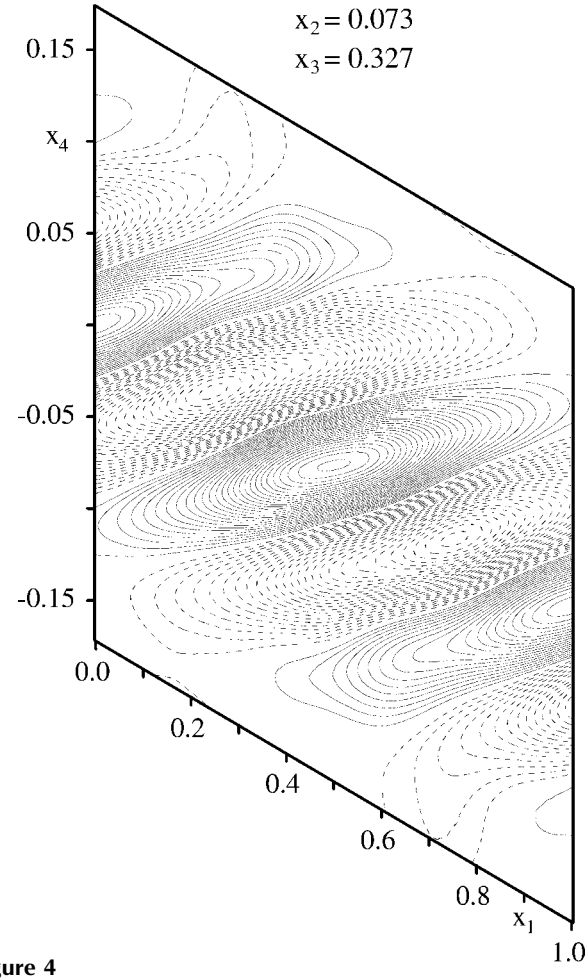

Figure 4
(x_1,x_4) section of the difference Fourier of $(LaS)_{1.13}TaS_2$ at the position of La2. Reflections phases were obtained from the refinement with Model A. Contours are at intervals of 2.5 e Å^{-3}, with solid lines for positive regions and dashed lines for negative regions.

Table 5
Modulation amplitudes for the temperature parameters in Model B of $(LaS)_{1.13}TaS_2$.

Shown are the amplitudes U^{ij}_{cn} and U^{ij}_{sn}.

	Ta1		La2	
	$n = 1$	$n = 2$	$n = 1$	$n = 2$
U^{11}_{cn}	0	−0.00058 (3)	−0.0013 (2)	−0.0070 (1)
U^{22}_{cn}		0.00018 (5)	−0.0025 (2)	−0.0021 (1)
U^{33}_{cn}	0	−0.00039 (5)	0.0011 (1)	−0.0025 (1)
U^{12}_{sn}		0.00006 (6)	−0.00782 (8)	0.0013 (2)
U^{13}_{sn}	0.00072 (4)	0	0.0020 (1)	−0.0020 (1)
U^{23}_{cn}	0.00028 (4)		0.00177 (7)	0.0000 (1)

uncertainties. Subsequent refinement of the occupation parameters for all atoms led to a substantial improvement of the partial R values of the main reflections from 0.022 to 0.018 for the TaS_2 subsystem and from 0.042 to 0.035 for the LaS subsystem. Only the occupancy of La2 became less than 1, while the occupancies of the other atoms remained equal to 1 within their standard uncertainties. This result strongly suggests that the La2 site contains a few per cent of vacancies. The introduction of modulation parameters for the occupancy of La2 led to further improvements of the fit. This result is selected as the best model of our analysis and it is denoted by Model B (Table 2). The refined parameters are summarized in Tables 4–6 and in deposited material. An alternative model for the occupation modulation with Crenel functions led to the same average occupancy, but with a less good fit to the satellite reflections than the harmonic model. Therefore, the harmonic modulation was selected as the best model. Apart from the lower R values, support for Model B comes from the Fourier map and difference Fourier (Figs. 5 and 6). For Model B the calculated positions of the atoms do follow the trace of maximum density in the Fourier map and the difference Fourier is now found to be nearly flat (Table 3). It is noticed that parameters that occur both in Model A and in Model B have values in these models that differ up to a maximum of a few times their standard uncertainties only.

Other attempts to obtain an improved structure model failed. The use of higher harmonics for the displacive modu-

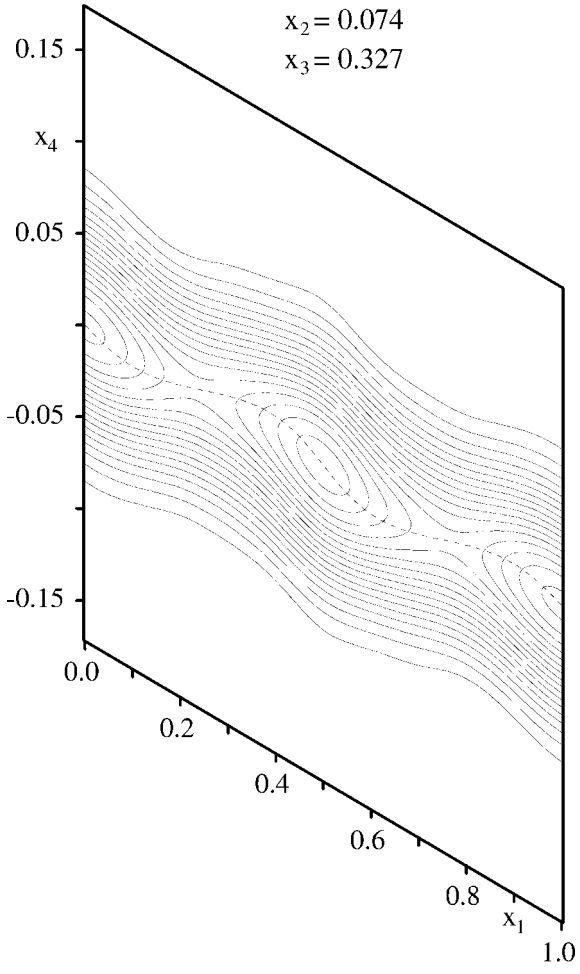

Figure 5
(x_1, x_4) section of the Fourier map of $(LaS)_{1.13}TaS_2$ at the position of La2. Reflection phases were obtained from the refinement with Model B. The contours are at intervals of 25 e Å^{-3}. The dashed line shows the positon of La(2) in the model.

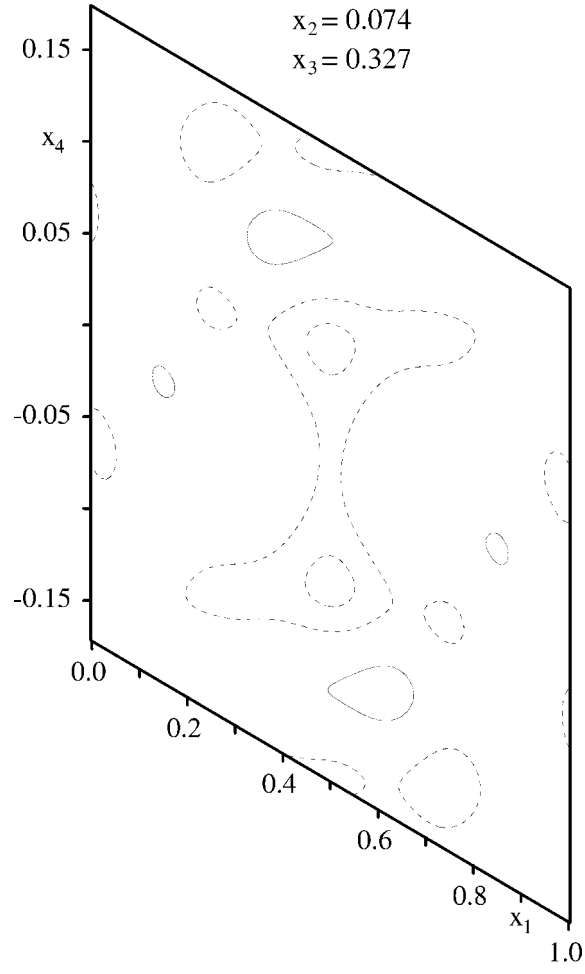

Figure 6
(x_1, x_4) section of the difference Fourier of $(LaS)_{1.13}TaS_2$ at the position of La2. Reflections phases were obtained from the refinement with Model B. Contours are at intervals of 2.5 e Å^{-3}, with solid lines for positive regions and dashed lines for negative regions.

Table 6
Parameters describing the occupational modulation of La2 in $(LaS)_{1.13}TaS_2$ and $(LaS)_{1.14}NbS_2$.

$p_{sn} = 0$ as determined by symmetry.

	p_o	p_{c1}	p_{c2}
$(LaS)_{1.13}TaS_2$	0.912 (2)	−0.030 (2)	0.0703 (8)
$(LaS)_{1.14}NbS_2$	0.949 (2)	−0.040 (1)	0.0671 (8)

lation causes no clear improvement of the R values and the calculated positions of the atoms no longer exactly follows the trace of the maximum density in the Fourier map. A third reason not to use higher harmonics is that no satellites of order higher than |2| were observed. Starting with Model A, the introduction of anharmonic displacement parameters for La2 and Ta1 did lead to lower R values for the main reflections, but not for the satellites. However, the probability density function (PDF) for both atoms had regions of significant negative values. From this it follows that anharmonic displacement parameters do not provide a suitable description of the structure. The introduction of modulation functions for the anharmonic displacement parameters led to even more negative values of the PDF.

Alternatively, the structure might have disorder in one of the subsystems. This was modelled by the introduction of a second position for the LaS layers obtained through translation along the incommensurate direction. The occupancies of both layers were restricted to sum up to 1. Refinement of the single occupancy parameter for a series of shift values never showed improvements of the R values and this model does not seem to be appropriate. Together with the previous result, which led to a partial occupancy of the La2 site but not of the S2 site, it further supports the model that vacancies exist only on the La2 site, and that the reduced scattering of the LaS subsystem is not due to disorder.

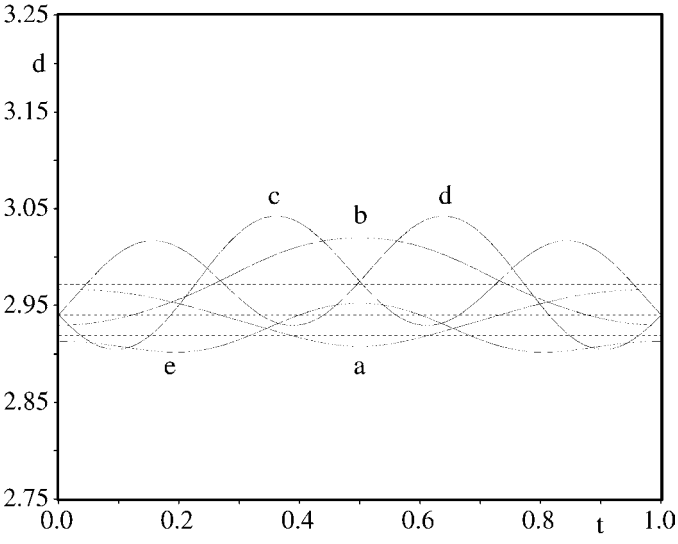

Figure 7
Coordination of La2 by the five nearest S2 atoms of the LaS subsystem in $(LaS)_{1.13}TaS_2$ as a function of t. The dashed lines represent the distances in the average structure. The solid lines show the distances in the modulated structure (Model B). For a description of the atoms a–e, see Table 10.

Table 7
R values for the refinement of Model C and Model D for $(LaS)_{1.14}NbS_2$.

	Model C		Model D	
Reflection group	R(obs)	wR(obs)	R(obs)	wR(obs)
All	0.073	0.137	0.048	0.080
Main	0.042	0.069	0.034	0.057
Main (NbS_2)	0.036	0.050	0.024	0.041
Main (LaS)	0.045	0.078	0.039	0.066
Common	0.050	0.078	0.041	0.056
Satellites $m = 1$	0.148	0.178	0.092	0.121
Satellites $m = 2$	0.268	0.381	0.113	0.121

3.2.2. $(LaS)_{1.14}NbS_2$. The refinements of $(LaS)_{1.14}NbS_2$ proceeded along the same lines as the refinement of $(LaS)_{1.13}TaS_2$ and similar features were observed. As for $(LaS)_{1.13}TaS_2$ the reflections $(2, K, L, -14)$ were excluded from the refinements. Model C for $(LaS)_{1.14}NbS_2$ is the counterpart of Model A for the structure of $(LaS)_{1.13}TaS_2$. The partial R value for the second-order satellites is especially worse than in the case of $(LaS)_{1.13}TaS_2$ (Table 7). The Fourier map and the difference Fourier exhibit the same problems as were found for $(LaS)_{1.13}TaS_2$ (Table 3).

The best fit to the data of $(LaS)_{1.14}NbS_2$ was obtained with Model D, which is Model B for $(LaS)_{1.13}TaS_2$, albeit with different values for the parameters. In the difference Fourier the strong peaks decreased by a factor of approximately 5. For the modulation parameters of the temperature factors of Nb1, significant values could not be obtained. One reason is that the scattering power of Nb is much lower than that of Ta and thus the parameters of Nb1 will be determined less accurately than the parameters of Ta1. Furthermore, it indicates that the modulation of the temperature factor of Nb1 will be a small effect, as was already found for the modulation of the temperature parameters of Ta1 in $(LaS)_{1.13}TaS_2$. In Model D the modulation parameters for the temperature factor of Nb(1) were set equal to zero. The results for the refined parameters in Model D are listed in Tables 6, 8 and 9, plus deposited material.

4. Discussion

We have determined accurate structure models for the modulated structure of $(LaS)_{1.14}TaS_2$ at room temperature and for the modulated structure of $(LaS)_{1.13}NbS_2$ at T = 115 K. Despite numerical differences that go well beyond the standard uncertainties, the general trends in the two structure models are the same. As expected, the temperature parameters for the structure at 115 K are smaller than for the structure at room temperature, but the anisotropy of the corresponding tensors is similar. This shows that the incommensurateness is resolved in the same way in both compounds and that the sizes of the modulations hardly depend on the temperature in the range 100–300 K.

Comparison with the previous study on the room-temperature structure of $(LaS)_{1.13}NbS_2$ (van Smaalen, 1991*b*)

Table 8
Displacement modulation parameters for Model D of $(LaS)_{1.14}NbS_2$.

Shown are the amplitudes A_{ni} and B_{ni} multiplied by the corresponding lattice parameter a_{vi} (Å). $A_{n2} = A_{n3} = B_{n1} = 0$ (n = 1,2), as determined by symmetry.

	$a_{v1}B_{11}$	$a_{v2}A_{12}$	$a_{v3}A_{13}$	$a_{v1}B_{21}$	$a_{v2}A_{22}$	$a_{v3}A_{23}$
Nb1	0	0	−0.0081 (3)	−0.0284 (2)	−0.0048 (3)	
S1	0.0255 (9)	−0.0129 (4)	−0.0060 (8)	0.0388 (5)	−0.0094 (9)	−0.0295 (4)
La2	0.0118 (4)	0.0910 (2)	−0.0195 (2)	−0.0479 (2)	−0.0023 (7)	0.0067 (3)
S2	−0.007 (1)	0.0545 (6)	0.006 (1)	0.0186 (7)	−0.021 (2)	0.0064 (8)

Table 9
Modulation amplitudes for the temperature parameters in Model D of $(LaS)_{1.14}NbS_2$.

Shown are the amplitudes U^{ij}_{cn} and U^{ij}_{sn}.

	La2	
	n = 1	n = 2
U^{11}_{cn}	−0.0023 (1)	−0.00317 (7)
U^{22}_{cn}	−0.0017 (2)	−0.00052 (9)
U^{33}_{cn}	0.00140 (9)	−0.00213 (7)
U^{12}_{sn}	−0.00458 (5)	0.0001 (2)
U^{13}_{sn}	0.00149 (9)	−0.00236 (6)
U^{23}_{cn}	0.00169 (4)	−0.0008 (1)

Table 10
Selected interatomic distances in $(LaS)_{1.13}TaS_2$ (Å).

Within the second subsystem, for each La—S2 contact in the first coordination sphere of La, the minimum and maximum values as well as their difference is given. The names of the atoms refer to Fig. 7. For the contact between the subsystems the shortest La—S1 distances are given at selected t values (for a definition of A_i and B see Fig. 8).

	d_{min}	d_{max}	Δd
La2—S2^{i}	2.2.908 (4)	967 (4)	0.059 (6)
La2—S2^{ii}	2.930 (4)	3.020 (4)	0.090 (6)
La2—S2^{iii}	2.904 (2)	3.0423 (6)	0.138 (2)
La2—S2^{iv}	2.904 (2)	3.0423 (6)	0.138 (2)
La2—S2^{v}	2.902 (2)	2.952 (3)	0.050 (4)
La2—S1^{vi}	2.868 (2) [A_1]	2.945 (4) [B]	0.077 (5)
La2—S1^{vii}	2.896 (2) [A_2]	2.945 (4) [B]	0.049 (5)

Symmetry codes: (i) $x_1, -1+x_2, x_3, x_4$; (ii) x_1, x_2, x_3, x_4; (iii) $-\frac{1}{2}+x_1, -\frac{1}{2}+x_2, x_3, \frac{1}{2}+x_4$; (iv) $\frac{1}{2}+x_1, -\frac{1}{2}+x_2, x_3, \frac{1}{2}+x_4$; (v) $x_1, -\frac{1}{2}+x_2, \frac{1}{2}-x_3, x_4$; (vi) $\frac{1}{2}+x_1, x_2, \frac{1}{2}-x_3, \frac{1}{2}+x_4$; (vii) $x_1, -\frac{1}{2}+x_2, \frac{1}{2}-x_3, 1+x_4$.

shows that the parameters for the displacive modulation have similar trends (Tables 4 and 8). However, the present refinements are much more accurate, with standard uncertainties less than 0.001 Å compared with standard uncertainties up to 0.04 Å in the previous study. This results in significantly non-zero values for all modulation parameters in the present study, while in the previous study only significantly non-zero values could be obtained for the modulation parameters of the atoms La and S1. Accordingly, the relative contributions to the modulation can now be estimated for all atoms.

In both structures the largest modulation amplitudes are found for La2, describing displacements parallel to the layers of up to 0.09 Å. The next largest amplitude (0.055 Å) is found for S2 and it describes a displacement along **b**. Almost the same value (0.045 Å) is found for S1. Since the bonding between La2 and S1 represents the contact between the two mutually incommensurate subsystems, the modulations of these two atoms are responsible for resolving the strain at this contact. The modulation of S2 can be interpreted as due to the elastic coupling towards La2. Nb1 and Ta1 have the smallest modulation amplitude (0.026 Å) and this value is due to the elastic coupling of these atoms towards S1.

The analysis of the variation of the environments of the atoms in an incommensurate structure can be performed by a so-called t plot (van Aalst *et al.*, 1976; van Smaalen, 1991*b*, 1995). Interatomic distances, site occupation values or temperature parameters are displayed as a function of t. All values that occur anywhere in the structure are thus displayed in one period along the t coordinate. An important property of the t plots is that the distances, temperature factors or other properties which are calculated at one value of t do represent these values at one position in physical space somewhere in the crystal. That is, the t plots allow the study of the correlations between the different modulations.

The distances between La2 and neighbouring S atoms are shown in Fig. 7 for the S2 atom in its own subsystem, and they are shown in Fig. 8 for the S1 atom of the TS_2 subsystem. A similar behaviour is found for both $(LaS)_{1.13}TaS_2$ and $(LaS)_{1.14}NbS_2$. Minimum and maximum values for these distances and their differences are collected in Tables 10 and 11.

The comparison of these figures with the corresponding plots in van Smaalen (1991*b*) show a similar trend. However, the range of distances obtained with the more accurate

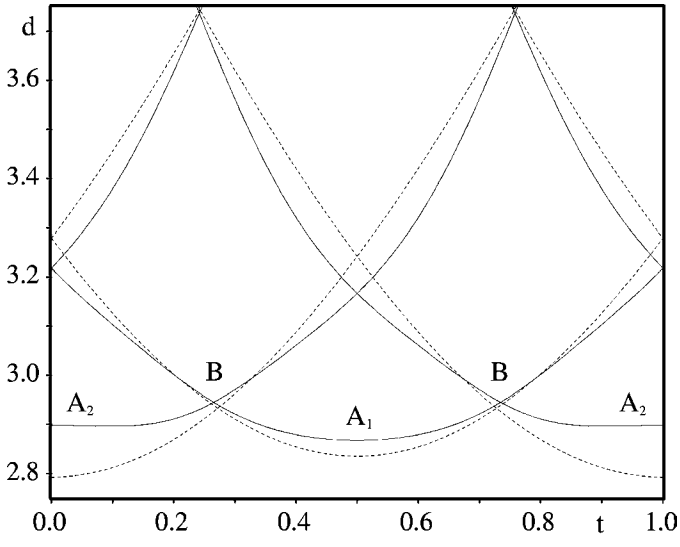

Figure 8
Coordination of La2 by the nearest S1 atom of the other subsystem in $(LaS)_{1.13}TaS_2$ as a function of t. The dashed lines represent the distances in the average structure. The solid lines show the distances in the modulated structure (Model B). For S1a the minimum distance to La2 is at A_1 (t = 0.5), for S1b the minimum distance to La2 is at A_2 (t = 0). At B S1a and S2b have the same distance to La2.

Table 11
Selected interatomic distances in $(LaS)_{1.14}NbS_2$.

Within the second subsystem, for each La—S2 contact in the first coordination sphere of La, the minimum and maximum values as well as their difference is given. For the contact between the subsystems the shortest La—S1 distances are given at selected t values (*cf.* Fig. 8). Symmetry operators were applied to the coordinates of the sulfur atoms as given in Table 10.

	d_{min}	d_{max}	Δd
La2—S2^{i}	2.901 (2)	2.973 (3)	0.072 (4)
La2—S2^{ii}	2.945 (3)	3.034 (1)	0.089 (3)
La2—S2^{iii}	2.912 (1)	3.0254 (4)	0.113 (1)
La2—S2^{iv}	2.912 (1)	3.0254 (4)	0.113 (1)
La2—S2^{v}	2.897 (1)	2.938 (2)	0.041 (2)
La2—S1^{vi}	2.877 (2) [A_1]	2.946 (4) [B]	0.069 (5)
La2—S1^{vii}	2.895 (2) [A_2]	2.946 (4) [B]	0.051 (5)

modulation parameters is smaller than obtained previously. In particular, the shortest La—S distance is now found to occur between the subsystems and the variation of this shortest distance is much smaller than previously found. It shows that the value of approximately 2.87 Å can be considered as the absolute minimum for the bonding distance between La and S atoms. It suggests that the driving force for the modulation is to resolve intersubsystem contacts that are too short (Fig. 8).

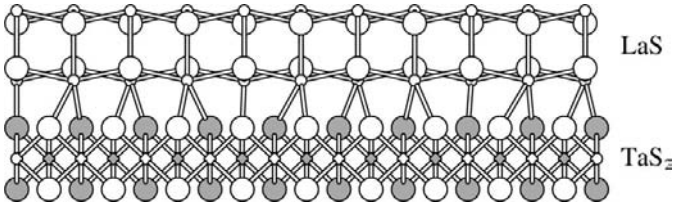

Figure 9
Projection along the common b axis of the structure of $(LaS)_{1.13}TaS_2$. Large circles represent S atoms, small circles denote metal atoms. Shaded and white circles denote atoms at different x_1 coordinates. The coordination of La2 is found to depend on the position in space.

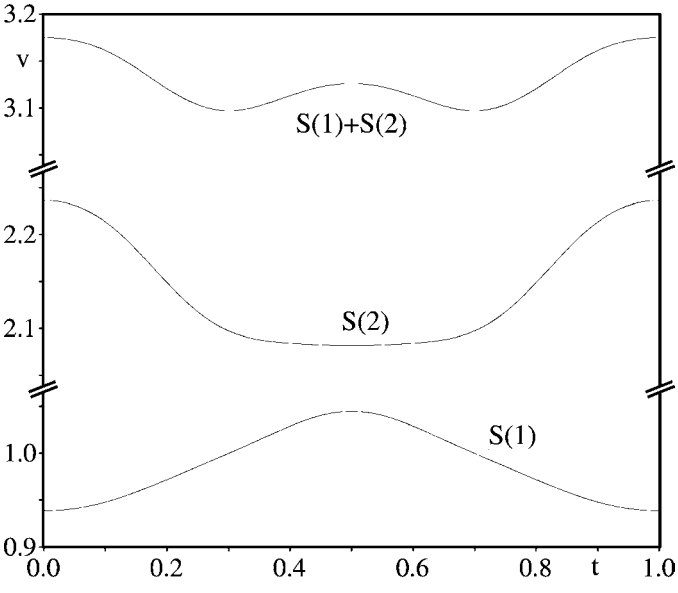

Figure 10
Valence of La2 in $(LaS)_{1.13}TaS_2$ as a function of t. Valence values were computed by the bond-valence method using the structure Model B and the bond-valence parameters R^0[La—S] = 2.64 Å and b = 0.37 Å (Brese & O'Keeffe, 1991).

Despite the fact that the more accurate modulation parameters show a more smooth character of the distances around La, an important variation of the local environment around this atom remains. Individual La—S distances vary up to 0.138 Å for $(LaS)_{1.13}TaS_2$ (Table 10) and 0.113 Å for $(LaS)_{1.14}NbS_2$ (Table 11). The coordination of La2 changes between 5 + 1 for $t = 0$ and $t = 0.5$ and 5 + 2 for $t = 0.25$ and $t = 0.75$. These variations in coordination can also be seen in the real space projection of the structure along **b** (Fig. 9). Concerning the valence states of the atoms, these variations compensate each other to a large extent (van Smaalen, 1992*b*). This is already suggested by the t plots of the distances, which show that a minimum in one distance is accompanied by a maximum in another distance. Fig. 10 shows the valence of La computed by the bond-valence method from the present structure model for $(LaS)_{1.13}TaS_2$. The total variation of the valence is found to be 0.078 for $(LaS)_{1.13}TaS_2$ and 0.049 for $(LaS)_{1.14}NbS_2$, and it is substantially smaller than the variation of the valence obtained with the less accurate structure model (van Smaalen, 1992*b*). Nevertheless, with significant values for the modulation parameters of all atoms, a small variation of the valence remains, which apparently is not resolved by the displacive modulation. Instead, a minimum valence value is found for $t = 0.3$ and $t = 0.7$, which is in the region of a 5 + 2 coordination of La (points B in Fig. 8), whereas a maximum valence is found for environments of La corresponding to 5 + 1 coordination (points A in Fig. 8). This means that the lowest valence corresponds to the points with the highest intersubsystem bonding.

The temperature parameters of La2 are plotted as a function of t in Figs. 11 and 13. For both compounds, all diagonal components as well as the equivalent isotropic parameter show a similar behaviour with maximum values for $t = 0.25$

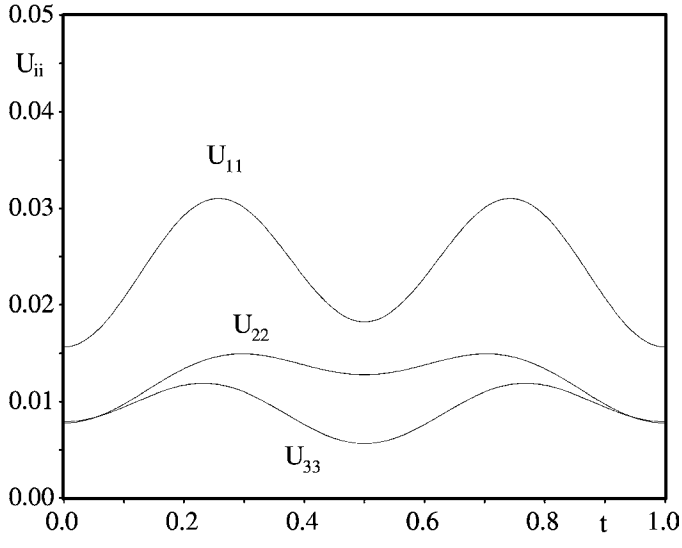

Figure 11
The temperature factors of La2 in $(LaS)_{1.13}TaS_2$ as a function of t for Model B.

and $t = 0.75$, and minimum values for $t = 0$ and $t = 0.5$. As noted before, the temperature parameters for the structure at $T = 115$ K are approximately a factor of two smaller than the parameters for the room-temperature structure, but they are positive for all values of t.

The t plot of the occupancy of the La(2) sites is shown in Figs. 12 and 14. It exhibits maxima at $t = 0$ and $t = 0.5$ and it has minimum values at $t = 0.25$ and $t = 0.75$. A possible numerical correlation between temperature parameters and occupation parameters in the refinement would combine larger temperature parameters (*i.e.* reduced scattering) with larger values for the occupancy (*i.e.* increased scattering). However, the opposite is found, where at the same t values either both the temperature parameters and occupancy values are larger than average or both are smaller than average. This absence of correlation effects between the two parameters gives additional support to the significance of the parameters in Models B and D.

Structurally, the t plots show that the highest valence (represents the tightest environment) corresponds to a minimum of the temperature parameter. That is, in the tightest environment the distribution of positions of the atoms is the smallest, in accordance with the general understanding of the chemical bond. Noteworthy is that these tightest environments also have the highest occupancy factors. This can be interpreted as the atoms prefer the sites with the stronger bonding.

As suggested by Rouxel *et al.* (1994), charge balance for a misfit layer compound $(MX)_{1+x}TX_2$ is only fulfilled if the site of M is not fully occupied. Using formal valences La^{3+} and T^{3+}, and the observed lattice constants, we obtain an expected average occupancy for the La site of 0.96 for both compounds. For $(LaS)_{1.14}NbS_2$ we find a value of 0.949 (2) (Table 6), which is in agreement with the expected value. For $(LaS)_{1.13}TaS_2$ we find 0.91. We do not have an explanation for the discrepancy between the theoretical and experimental values in this case.

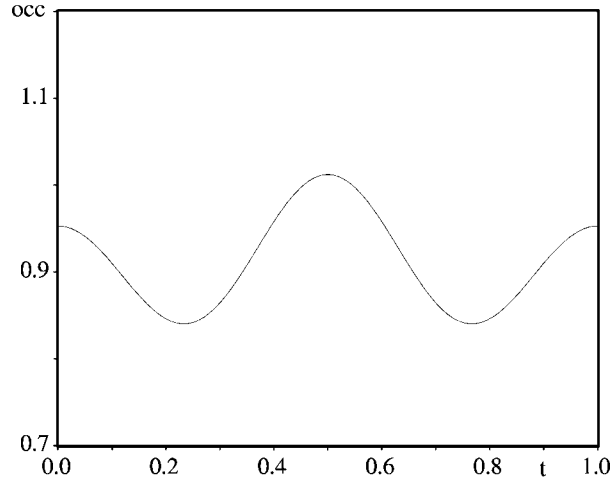

Figure 12
The occupation of the La2 site in $(LaS)_{1.13}TaS_2$ as a function of t for Model B.

5. Conclusions

We have determined accurate structure models for the modulated structures of the inorganic misfit layer compounds $(LaS)_{1.13}TaS_2$ and $(LaS)_{1.13}NbS_2$. The analysis shows that the modulations are almost equal between these two compounds and that they are almost independent of temperature. The correlation is determined between the incommensurate contact between the two subsystems, the displacive modulation, the temperature parameters and the modulation of the partial occupancy of the La sites. It is found that a tighter environment corresponds to smaller temperature factors, but larger values for the occupancy. This is to be understood by the fact that the La atoms are attracted to the sites with the higher bonding.

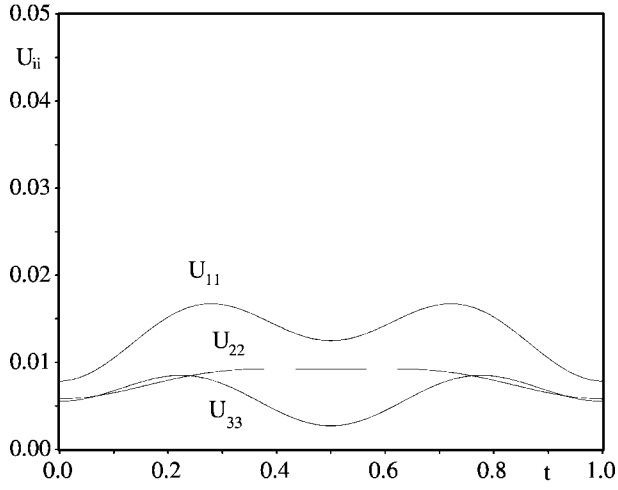

Figure 13
The temperature factors of La2 in $(LaS)_{1.14}NbS_2$ as a function of t for Model D.

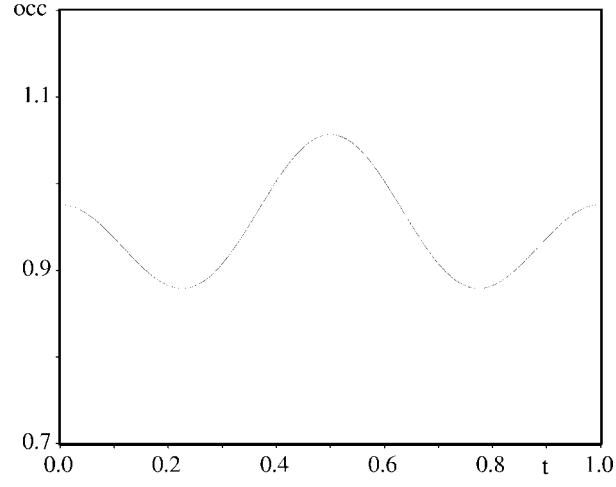

Figure 14
The occupation of the La2 site in $(LaS)_{1.14}NbS_2$ as a function of t for Model D.

This research has been made possible by financial support from the Deutsche Forschungsgemeinschaft (DFG).

References

Aalst, W. van, den Hollander, J., Peterse, W. J. A. M. & de Wolff, P. M. (1976). *Acta Cryst.* B**32**, 47–58.

Becker, P. J. & Coppens, P. (1974). *Acta Cryst.* A**30**, 129–152.

Boer, J. L. de, Meetsma, A., Zeinstra, T. J., Haange, R. J. & Wiegers, G. A. (1991). *Acta Cryst.* C**47**, 924–930.

Brese, N. E. & O'Keeffe, M. (1991). *Acta Cryst.* B**47**, 192–197.

Herrendorf, W. (1993). *HABITUS*. PhD thesis. Universität Giessen.

Janssen, T., Janner, A., Looijenga-Vos, A. & de Wolff, P. M. (1999). *International Tables for Crystallography*, Vol. C, 2nd ed. Dordrecht: Kluwer Academic Publishers.

Jobst, A. & van Smaalen, S. (2001). Unpublished.

Kuypers, S. & van Landuyt, J. (1992). *Mater. Sci. Forum*, **100–101**, 223–272.

Meerschaut, A., Rabu, P. & Rouxel, J. (1989). *J. Solid State Chem.* **78**, 35–45.

Meetsma, A. & Spek, T. (1996). *HELENA*. Chemical Physics, University of Groningen, The Netherlands.

Petříček, V. & Dušek, M. (1998). *JANA*98. Institute of Physics, Praha, Czech Republic.

Rouxel, J., Moëlo, Y., Lafond, A., DiSalvo, F. J., Meerschaut, A. & Roesky, R. (1994). *Inorg. Chem.* **33**, 3358–3363.

Smaalen, S. van (1991*a*). *Phys. Rev. B*, **43**, 11330–11341.

Smaalen, S. van (1991*b*). *J. Phys. Condens. Matter*, **3**, 1247–1263.

Smaalen, S. van (1992*a*). *Mater. Sci. Forum*, **100–101**, 173–222.

Smaalen, S. van (1992*b*). *Acta Cryst.* A**48**, 408–410.

Smaalen, S. van (1995). *Cryst. Rev.* **4**, 79–202.

Smaalen, S. van (1999*a*). *Computational Studies of New Materials*, edited by D. A. Jelski & T. F. George. Singapore: World Scientific.

Wiegers, G. A. (1996). *Prog. Solid State Chem.* **24**, 1–139.

Wiegers, G. A., Meetsma, A. R. J., Haange, S. v. S. & de Boer, J. L. (1990). *Acta Cryst.* B**46**, 324–332.

Wolff, P. M. de, Janssen, T. & Janner, A. (1981). *Acta Cryst.* A**37**, 625–636.